

# CH<sub>2</sub> + CO<sub>2</sub> → CH<sub>2</sub>O + CO, One-Step Oxygen Atom Abstraction or Addition/Fragmentation via α-Lactone?

Dalila Kovacs\* and James E. Jackson\*

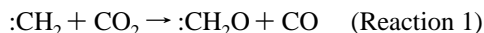
Department of Chemistry, Michigan State University, East Lansing, Michigan 48824-1322

Received: September 27, 2000; In Final Form: May 7, 2001

Ab initio G2 calculated pathways are presented for the reaction  $\text{CH}_2 + \text{CO}_2 \rightarrow \text{CH}_2\text{O} + \text{CO}$  in which net transfer of a double bonded oxygen atom occurs from  $\text{CO}_2$  to the carbene. Of particular interest are the electronic state of the attacking methylene, the structure of the possible intermediates, and the lowest energy path(s) available for this reaction. As expected, our results support the assignment of  $\alpha$ -lactone **1** as the intermediate observed by IR in the matrix isolation experiments of Milligan and Jacox; analogous reactions involving substituted carbenes have more recently been reported by Sander et al. We obtain  $\Delta H_f^\circ(\mathbf{1}) = -43.3$  kcal/mol based on the G2 atomization energy, while a variety of isodesmic reactions point to slightly higher values (averaged  $-42.7$  kcal/mol). Acyclic  $\cdot\text{CH}_2\text{O}(\text{CO})\cdot$  (methylene-oxycarbonyl) and  $\cdot\text{CH}_2\text{CO}_2\cdot$  (acetoxy) biradicals **2** and **3**, respectively, were also considered on both singlet and triplet potential energy surfaces. According to the calculations, the singlet reaction proceeds with little or no barrier to form **1**; subsequent ring fragmentation ( $\Delta H^\ddagger = 27.5$  kcal/mol) yields the products  $\text{CH}_2\text{O} + \text{CO}$ . Collision orientation must play a role, however; Wagner et al. have reported that reaction is only half as fast as collisional deactivation of  $^1\text{CH}_2$  to  $^3\text{CH}_2$  which presumably occurs via nonproductive encounter geometries. An activated channel ( $\Delta H^\ddagger = 23.2$  kcal/mol) was also located in which  $^1\text{CH}_2$  directly abstracts oxygen from  $\text{CO}_2$  via an ylide-like TS **12**. The lowest energy  $^3\text{CH}_2 + \text{CO}_2$  attack is endothermic by 7.8 kcal/mol, forming the triplet acetoxy diradical **33**; a higher energy path leads to methylene-oxycarbonyl diradical **32**. Barriers for these two processes are  $\Delta H^\ddagger = 19.3$  and  $57.7$  kcal/mol, respectively. No path for isomerization of **33** to **32** was found. Attempts to locate regions on the triplet approach surface where the singlet crosses to become the lower energy spin state were complicated by the difficulty of optimizing geometries within the composite G2 model. Preliminary efforts, however, indicate that such crossings occur at geometries higher in energy than separated  $^1\text{CH}_2 + \text{CO}_2$ , suggesting that their role should be relatively unimportant in this reaction.

## Introduction

The first reported abstraction of a double bonded oxygen atom by a carbene<sup>1</sup> was the gas-phase reaction of methylene,  $:\text{CH}_2$ , with carbon dioxide,  $\text{CO}_2$ :



The present computational analysis of reaction 1 was prompted by our own recent studies of oxygen transfer from carbonyl compounds to carbenes.<sup>2</sup> Of particular mechanistic interest is the potential existence of a single-step “pluck” reaction<sup>3</sup> in which pairs of bonds are simultaneously broken and formed. The results also shed light on the recent suggestion, by Naito, et al., of  $\text{O}=\text{C}=\text{O}^+-\text{CRR}'^-$  ylide formation.<sup>4</sup>

## Background

Reaction 1 was first observed in 1958. Kistiakowsky et al., studying the reaction of methylene generated from ketene, noted excess CO production when  $\text{CO}_2$  was used as an “inert” buffer gas. They proposed that the attack of triplet methylene on  $\text{CO}_2$  forms an intermediate,  $\alpha$ -lactone (**1**), which decomposes to formaldehyde and CO (see Figure 1).

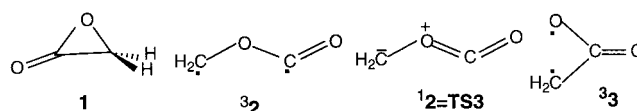
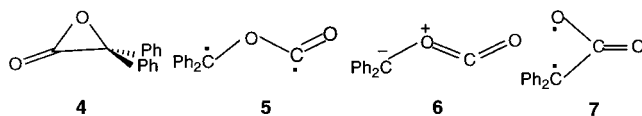


Figure 1. Potential intermediates in the  $:\text{CH}_2 + \text{CO}_2$  reaction.

A few years later, in 1962, Milligan and Jacox<sup>5</sup> photolyzed diazomethane in a  $\text{CO}_2$  matrix, at ca. 50 K. Monitoring by infrared (IR) spectroscopy, these authors observed a set of absorptions that grew as those from the initially generated  $:\text{CH}_2$  decreased. A particularly strong band at  $>1900$   $\text{cm}^{-1}$ , combined with isotopic labeling results,<sup>6</sup> led to a tentative assignment of the new species as the  $\alpha$ -lactone **1**, in which the carbonyl stretch is blue-shifted due to the ring strain. At the time, however, acyclic diradical intermediates such as **32** or **33** were not ruled out.

In 1977, almost two decades after Kistiakowsky's initial experiment, Laufer and Bass<sup>7</sup> studied the kinetics of Reaction 1 by flash photolysis with  $\text{CH}_2\text{N}_2$  and  $\text{CH}_2\text{CO}$  as methylene precursors. The rate constant obtained for this reaction was  $3.3 \times 10^{-14}$   $\text{cm}^3$  molecule<sup>-1</sup> s<sup>-1</sup>, based on known values for triplet methylene dimerization ( $k = 5.3 \times 10^{-11}$   $\text{cm}^3$  molecule<sup>-1</sup> s<sup>-1</sup>) and its reaction with acetylene ( $k = 7.5 \times 10^{-12}$   $\text{cm}^3$  molecule<sup>-1</sup> s<sup>-1</sup>). Although the latter rate constant has since been revised,<sup>8</sup> Laufer's results correctly describe a slow reaction between  $^3\text{CH}_2$  and  $\text{CO}_2$ .

\* Authors to whom correspondence should be addressed.



**Figure 2.** Potential intermediates in the  $:\text{CPh}_2 + \text{CO}_2$  reaction.

In the same year, Hsu and Lin<sup>9</sup> determined the vibrational energy of the carbon monoxide released from reaction 1, monitoring its production with a continuous wave CO laser. Methylene was generated by photolysis of  $\text{CH}_2\text{I}_2$  ( $\lambda > 210$  nm). The vibrational state population of CO produced was found to be close to that predicted by statistical calculations, assuming a long-lived  $\text{CH}_2\text{CO}_2$  intermediate,<sup>10</sup> and a total final vibrational energy of 63 kcal/mol (the overall reaction's exothermicity). The authors found that product CO is vibrationally excited up to  $\nu = 4$ , carrying an average of 1.9 kcal/mol. By extrapolation to the previously reported reaction rate, the authors assigned the singlet electronic state to the reacting methylene, but cited Laufer's then-unpublished work, indicating that triplet methylene might also be responsible for the oxygen abstraction.

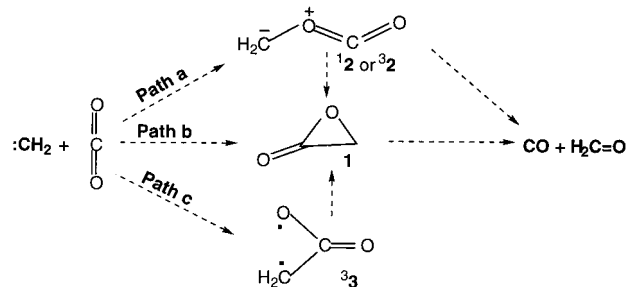
Sophisticated new techniques allowed Wagner et al.<sup>11</sup> in 1990, to perform detailed kinetic measurements on reaction 1. Methylene, generated by laser photolysis of ketene, was observed by laser-induced fluorescence ( $^1\text{:CH}_2$ ) and laser magnetic resonance ( $^3\text{:CH}_2$ ) allowing quantitative evaluation of intersystem crossing (ISC). The authors found that roughly 2/3 of  $^1\text{:CH}_2 + \text{CO}_2$  collisions cause  $^1\text{:CH}_2$  to relax to  $^3\text{:CH}_2$ ; for the remaining 1/3, three exothermic reaction channels were considered, leading to the formation of glyoxal  $\text{HCOCHO}$ ,  $\text{H}_2 + 2\text{CO}$ , or  $\text{H}_2\text{CO} + \text{CO}$ . Preliminary experiments in Wagner's lab showed that the  $^3\text{:CH}_2 + \text{CO}_2$  reaction is very slow, even at higher temperatures.<sup>12</sup> Furthermore, the products may only be the result of collisional activation of  $^3\text{:CH}_2$  to  $^1\text{:CH}_2$ , which then reacts rapidly with  $\text{CO}_2$ . Wagner concluded that formaldehyde and CO are "the probable chemical products", and that  $\alpha$ -lactone is a "plausible intermediate".

Based on DeMore's observation<sup>13</sup> that diphenyldiazomethane photolysis in the presence of  $\text{O}_2$  generates benzophenone, Sander<sup>14</sup> investigated the role of  $:\text{CPh}_2$  as an "oxygen abstractor" from  $\text{CO}_2$  doped into Ar or Xe matrixes. The observed intermediate has a high-frequency carbonyl stretch ( $1890\text{ cm}^{-1}$ ) and it fragments upon UV irradiation ( $\lambda > 220$  nm), to  $\text{Ph}_2\text{CO}$  and CO. It is thus assigned as diphenyloxiranone **4**. The spin forbidden reaction of the ground state  $^3\text{:CPh}_2$  with  $\text{CO}_2$  to form **4** shows a thermal barrier, occurring only when the matrix is annealed to 35 K.<sup>15</sup> Photoexcited  $:\text{CPh}_2$ , however, reacts rapidly above 10 K to yield the same products, perhaps due to the availability of a low lying empty p orbital, as in the singlet case. No direct evidence was obtained for diradical or zwitterionic intermediates such as **5**, **6**, or **7**, the diphenyl analogues of **2** or **3** (see Figure 2).

To clarify the carbene characteristics responsible for oxygen abstraction, Sander et al. studied the reaction of  $\text{CO}_2$  with four carbenes,<sup>16</sup> two with triplet and two with singlet ground states.<sup>17</sup> They found no indication that carbene reactivity is influenced by the spin state. Instead, the "philicity" of the carbene appears to control the oxygen abstraction via rate-determining nucleophilic attack on the  $\text{CO}_2$  carbon. With the available data, it was impossible to determine whether the reaction is concerted or not.

Reaction 1 has also been noted by Chateauneuf<sup>18</sup> in a laser flash photolysis study of  $:\text{CPh}_2$  in supercritical  $\text{CO}_2$ . The  $:\text{CPh}_2$ , generated by photolysis from diphenyldiazomethane, "most likely" forms diphenyl  $\alpha$ -lactone. The state selectivity of the

### SCHEME 1: Possible Reaction Paths



carbene is unclear, no differentiation being made between the "spin allowed" concerted addition of the singlet and the "spin forbidden" formation of the lactone through the triplet manifold, via a diradical intermediate.

In a theoretical study by Davidson et al.<sup>19</sup> exploring gas-phase dissociation of chloroacetyl anion, three possible products of chloride anion loss were considered:  $\alpha$ -lactone (**1**), acetoxyl diradical ( $^3\mathbf{3}$ ), and a zwitterionic state of the dioxatrimethylenemethane, structure **3**. The lactone was found to be the most stable,<sup>20</sup> with the diradical 35 kcal/mol higher in energy. The zwitterion, upon optimization, collapsed to  $\alpha$ -lactone or separated into  $:\text{CH}_2$  and  $\text{CO}_2$ . From Davidson's calculation, Squires et al. estimated a heat of formation for  $\alpha$ -lactone **1** of  $-51$  kcal/mol, consistent with their later collision-induced dissociation (CID)<sup>21</sup> and subsequent tandem MS/CID experiments on several acetate anions.<sup>22</sup> These efforts yielded a heat of formation of  $\alpha$ -lactone of  $-47 \pm 4.7$  kcal/mol, a value that is also compatible with a more recent computational estimate ( $-45.2 \pm 2.5$  kcal/mol via two different isodesmic reactions)<sup>23</sup> and our own G2 value ( $-43.3$  kcal/mol). In a theoretical study of  $\alpha$ -hydroxycarboxylic acid decarboxylation,<sup>24</sup> the  $\Delta H^\ddagger$  value and TS structure for  $\alpha$ -lactone fragmentation into  $\text{CH}_2\text{O} + \text{CO}$  were very similar to our own (vide infra).

### Objectives

To address the question of methylene spin state in reaction 1, we began our theoretical investigation by looking at several modes of methylene attack on  $\text{CO}_2$  on both the singlet ( $^1\text{:CH}_2$ ) and triplet ( $^3\text{:CH}_2$ ) potential energy surfaces. We envisioned three possible paths (see Scheme 1):

**path a.** electrophilic attack at the oxygen lone pair of electrons, leading to an ylide-like intermediate **12**. The possibility of direct oxygen transfer via a  $^1\mathbf{2}$ -like TS to yield  $\text{CO} + \text{H}_2\text{CO}$  was investigated along with further cyclization of **12** to **1**;

**path b.** cycloaddition to a  $\text{C}=\text{O}$   $\pi$  bond, leading to the formation of  $\alpha$ -lactone **1**. Fragmentation of **1** then generates the final products  $\text{CO} + \text{H}_2\text{CO}$ ;

**path c.** radical-like attack at the C atom, leading to acetoxyl diradical  $^3\mathbf{3}$ . Further transformation of  $^3\mathbf{3}$  to **1** was considered, as no obvious direct path links  $^3\mathbf{3}$  to  $\text{CO} + \text{H}_2\text{CO}$ .

In the course of this work other questions were addressed: is there a direct path (concerted or stepwise) via an open ylide-like structure  $^1\mathbf{2}$  (transition state or intermediate), to  $\text{CO} + \text{H}_2\text{CO}$ ? Is  $\alpha$ -lactone **1** the observed intermediate in the early matrix studies? If so, is it formed in one step, **path b** above, or via cyclization of other species, such as  $^1\mathbf{2}$  or  $^3\mathbf{3}$ ? If attack occurs at carbon, **path c**, are there stable acetoxyl-like intermediates  $^3\mathbf{3}$ ? If so, would they close to  $\alpha$ -lactone **1**, or rearrange to diradicals  $^3\mathbf{2}$ ? If  $^3\text{:CH}_2$  reacts with  $\text{CO}_2$  to any significant degree, at what point does intersystem crossing (ISC) occur en route to closed-shell products **1** or  $\text{CO} + \text{H}_2\text{CO}$ ?

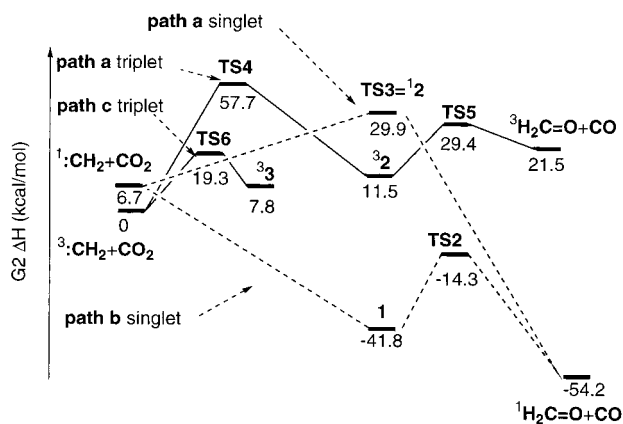


**Figure 3.** Enthalpy profiles at the G2 level. Solid lines represent connections between the intermediates and transition states on the triplet PES; dotted lines are used for the singlet PES.

**TABLE 1: Thermochemical Data for Reaction 1**

method	$\Delta H_{\text{rxn}}$ singlet	$\Delta H_{\text{rxn}}$ triplet
HF/6-31G* <sup>a</sup>	-61.3	16.8
zpe//HF/6-31G*	+2.6	-0.7
MP2/6-31G*//HF/6-31G* <sup>a</sup>	-69.8	32.7
MP4/6-31G*//HF/6-31G* <sup>a</sup>	-69.2	24.5
MP2/6-31G*//MP2/6-31G* <sup>a</sup>	-69.7	34.1
zpe//MP2/6-31G*	+2.1	-0.8
G2 enthalpy	-60.8	21.5
experimental <sup>b</sup>	-61	23.8

<sup>a</sup> Corrected for zero-point energy. <sup>b</sup> Calculated from experimental  $\Delta H_f$  (kcal/mol): <sup>3</sup>:CH<sub>2</sub> 92.35; <sup>1</sup>:CH<sub>2</sub> 101.35; CO<sub>2</sub> -94.05 ± 0.03; CO -26.42 ± 0.04; <sup>1</sup>H<sub>2</sub>CO -27.70; and <sup>3</sup>H<sub>2</sub>CO 73.9 from Hertzberg, G. *Electronic Spectra of Polyatomic Molecules*; van Nostrand: Princeton, 1967.

## Methods and Procedures

All calculations were performed using the Gaussian 94 and 98 packages,<sup>25</sup> run on a cluster of Silicon Graphics computers. All stationary points were optimized and characterized by vibrational analysis at the HF/6-31G\* and MP2/6-31G\* levels. Additional energy calculations were run at the MP4/6-31G\*//MP2/6-31G\* level.<sup>26</sup>

Among the stationary points found, connections on the PES were verified by running intrinsic reaction coordinate (IRC) calculations,<sup>27</sup> starting in both directions from each TS at both the HF/6-31G\* and MP2/6-31G\* levels. Selected IRC points were analyzed as single points at the MP2/6-31G\*//HF/6-31G\* and MP4/6-31G\*//HF/6-31G\* levels. To better ascertain the presence or absence of stationary points on the surface for singlet methylene approaching CO<sub>2</sub>, B3LYP/6-31G\* and QCISD/6-31G\* optimizations were also carried out for this region of the singlet PES.

In an effort to obtain experimentally relevant energetics, we computed G2 energies for all stationary points. The G2<sup>28</sup> error between experimental and calculated values<sup>29</sup> for the singlet-triplet (S-T) gap in methylene is only 2.3 kcal/mol, much closer than with any of the other above-mentioned methods.<sup>30</sup>

## Discussion

**Thermochemistry.** The experimental<sup>31</sup> heats of reaction 1 on singlet and triplet PESs are compared in Table 1 with data from our ab initio calculations. Figure 3 displays the reactions' overall G2 energy profiles, which compare very well with experiment. Formation of triplet products (<sup>3</sup>CH<sub>2</sub>O + <sup>1</sup>CO) would be endothermic from either singlet or triplet starting points. Without extra activation, the reaction must therefore end on the

**TABLE 2: Relative<sup>a</sup> Energies of Intermediates**

ab initio method	<sup>1</sup> :CH <sub>2</sub> + CO <sub>2</sub>	<b>1</b>	<sup>3</sup> <b>1</b> <sup>b</sup>	<sup>1</sup> <b>2</b>	<sup>3</sup> <b>2a</b>	<sup>3</sup> <b>2s</b>	<sup>3</sup> <b>3p</b>	<sup>3</sup> <b>3s</b> <sup>c</sup>
NImag <sup>d</sup>		0	1	0	0	0	1	
HF/6-31G*//HF/6-31G*	30.8	-6.9	53.4	89.8	22.0	19.9	1.2	10.0
$\Delta zpe^e$ at HF/6-31G*	-0.3	7.0	5.4	3.2	4.1	4.4	4.0	3.3
MP2/6-31G*//HF/6-31G*	21.0	-40.6	55.4	31.2	5.2	4.7	14.3	22.1
MP4/6-31G*//HF/6-31G*	17.2	-40.0	50.0	27.7	3.6	3.4	8.4	16.5
MP2/6-31G*//MP2/6-31G*	20.9	-40.3		40.1	15.8	15.5	17.0	24.0
$\Delta zpe^e$ at MP2/6-31G*	-0.5	6.1		3.2	3.8	4.1	4.2	3.0
MP4/6-31G*//MP2/6-31G*	17.1	-39.7		36.2	14.2	14.2	11.7	18.8
MP2(full)/6-31G*	19.0	-40.9		39.8	15.8	15.5	16.9	24.1
QCISD(T,E4T)/6-311G(dp)	12.5	-36.7		36.8	13.3	13.3	9.2	18.1
G2 enthalpy	6.7	-41.8		29.9	11.5	12.0	7.8	16.4

<sup>a</sup> At each level of theory, the total energies for <sup>3</sup>:CH<sub>2</sub> + CO<sub>2</sub> were used for reference; total values, in hartrees, are as follows: HF/6-31G\*, -226.55568; zpe correction, 19.56 kcal/mol; MP2/6-31G\*//MP2/6-31G\*, -227.11114; zpe correction 18.5 kcal/mol; MP4/6-31G\*//MP2/6-31G\* -227.15240; from the series of G2 method iterations: MP2(full)/6-31G\*, -227.12580; QCISD(T, 4ET)/6-311G(dp), -227.26998; G2 enthalpy, -227.42297. <sup>b</sup> Optimization of triplet  $\alpha$ -lactone at MP2/6-31G\*//MP2/6-31G\*, <sup>3</sup>**1**, led to <sup>3</sup>**2a**. <sup>c</sup> Optimization at the HF/6-31G\* level of acetoxy staggered structure <sup>3</sup>**3s** as a singlet, leads to  $\alpha$ -lactone **1**. <sup>d</sup> NImag = the number of imaginary frequencies obtained by vibrational analysis at both HF and MP2 levels; NImag = 0 indicates minima on PESs, whereas NImag = 1 indicates transition states. <sup>e</sup>  $\Delta zpe$  is the difference between the zero-point energies of the species at the indicated level and the corresponding zpe of <sup>3</sup>:CH<sub>2</sub> + CO<sub>2</sub>.

singlet PES. The starting state is less clear; singlet carbene is generally thought to be the initial product formed from all the precursors used,<sup>32</sup> but collision-induced equilibration to the triplet ground state occurs readily, raising the possibility of intersystem crossing (ISC) before or during the <sup>1</sup>:CH<sub>2</sub>-CO<sub>2</sub> collision.

Among potential intermediates in this reaction, we have examined  $\alpha$ -lactone **1**, ylide <sup>1</sup>**2** (reabeled **TS3**; vide infra), diradical <sup>3</sup>**2**, and acetoxy diradical <sup>3</sup>**3** (Figure 1). Table 2 lists their energies, in kcal/mol, relative to <sup>3</sup>:CH<sub>2</sub> + CO<sub>2</sub>. A complete list, with calculated coordinates and total energies is available in the supporting material.

Figures 3-7 sketch the connectivity among the intermediates and transition states found.<sup>33</sup> Table 3 summarizes TS energies relative to <sup>3</sup>:CH<sub>2</sub> + CO<sub>2</sub>.

**Reaction Paths. path a, singlet PES.** This direct one-step path for oxygen abstraction (Figure 4) takes place via **TS3**, a stationary point like the structure expected for ylide <sup>1</sup>**2** (for which no minimum was found). The calculated barrier is dramatically lowered by inclusion of electron correlation; at HF, MP2, and G2 levels it is 62.5, 19.5, and 23.2 kcal/mol, respectively, above <sup>1</sup>:CH<sub>2</sub> + CO<sub>2</sub>. Likewise, the geometry of **TS3** changes significantly from HF to MP2 levels (Figure 4).

**path a, triplet PES.** In this two-step process (Figure 5), triplet methylene attacks one of the oxygen atoms of CO<sub>2</sub> via **TS4** to form <sup>3</sup>**2**. The high barrier and endothermicity of the initial attack (57.7 and 11.5 kcal/mol, respectively, at the G2 level) are expected, reflecting the difficulty of breaking a C=O double bond. Subsequent cleavage of <sup>3</sup>**2** via **TS5** leads to CO + <sup>3</sup>CH<sub>2</sub>O, a process for which the barrier and endothermicity are 17.9 and 10.0 kcal/mol, respectively. With its high barriers and an excited-state product (<sup>3</sup>CH<sub>2</sub>O), this path, as described, is

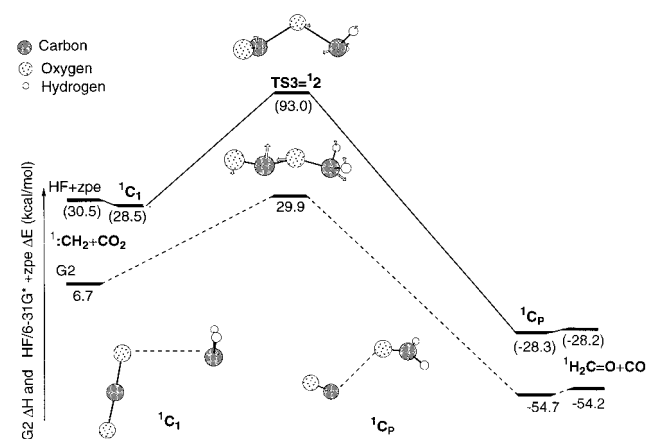
**TABLE 3: Relative<sup>a</sup> Energies of Transition States**

Singlet PES Connecting	<sup>1</sup> TS1 <sup>1</sup> R-1	<sup>1</sup> TS2 1- <sup>1</sup> P	<sup>1</sup> TS3 <sup>1</sup> R- <sup>1</sup> P
HF/6-31G**/HF/6-31G*	34.2	29.8	89.8
$\Delta$ zpe HF/6-31G*	3.3	1.7	3.2
MP2/6-31G**/HF/6-31G*	10.9	-5.9	31.2
MP4/6-31G**/HF/6-31G*	7.9	-7.9	27.7
MP2/6-31G**/MP2/6-31G*		-6.5	40.1
$\Delta$ zpe MP2/6-31G*		4.4	3.2
MP4/6-31G**/MP2/6-31G*		-8.6	36.2
MP2(full)/6-31G*		-6.2	39.8
QCISD(T,E4T)/6-311G(dp)		-5.5	36.8
G2 enthalpy		-14.3	29.9

Triplet PES connecting	<sup>3</sup> TS4 <sup>3</sup> R- <sup>3</sup> 2a	<sup>3</sup> TS5 <sup>3</sup> 2a- <sup>3</sup> P	<sup>3</sup> TS6 <sup>3</sup> R- <sup>3</sup> 3p	<sup>3</sup> TS7 <sup>3</sup> 3p- <sup>3</sup> 2a	<sup>3</sup> TSa-s <sup>3</sup> 2a- <sup>3</sup> 2s	<sup>3</sup> TSrot <sup>3</sup> 2s- <sup>3</sup> 2s
HF/6-31G**/HF/6-31G*	84.8	38.6	31.2	84.9	28.9	23.1
$\Delta$ zpe HF/6-31G*	2.3	2.3	1.1	4.6	3.6	3.8
MP2/6-31G**/HF/6-31G*	68.0	26.8	22.4	86.4	24.0	18.8
MP4/6-31G**/HF/6-31G*	63.3	20.2	19.2	80.5	22.0	17.9
MP2/6-31G**/MP2/6-31G*	68.6	41.6	29.3		25.7	20.3
$\Delta$ zpe MP2/6-31G*	2.3	1.9	1.9		3.6	3.3
MP4/6-31G**/MP2/6-31G*	65.2	38.9	24.3		23.9	18.5
MP2(full)/6-31G*	68.5	41.9	26.4		25.7	20.3
QCISD(T,E4T)/6-311G(dp)	63.3	29.5	19.3		21.9	18.5
G2 enthalpy	57.7	29.4	19.3		19.5	16.1

<sup>a</sup> Energy difference, in kcal/mol, with respect to the ground-state energy of CO<sub>2</sub> + <sup>3</sup>:CH<sub>2</sub>. <sup>1</sup>R = CO<sub>2</sub> + <sup>1</sup>:CH<sub>2</sub>; <sup>3</sup>R = CO<sub>2</sub> + <sup>3</sup>:CH<sub>2</sub>; <sup>1</sup>P = H<sub>2</sub>CO + <sup>1</sup>:CH<sub>2</sub>.



**Figure 4.** Path a on singlet PES. The G2 enthalpies and ZPE corrected HF/6-31G\*\*/HF/6-31G\* energies (in parentheses) are referenced to <sup>3</sup>:CH<sub>2</sub> + CO<sub>2</sub> as 0 kcal/mol. The geometries of complex <sup>1</sup>C<sub>1</sub>, complex <sup>1</sup>C<sub>p</sub> and TS3 = <sup>1</sup>2 are represented. For TS3 both HF and MP2 (i.e., G2) geometries are shown, with arrows indicating the imaginary vibration which corresponds to the reaction coordinate.

endothermic and unlikely to play any role in the :CH<sub>2</sub> + CO<sub>2</sub> reaction.

*path b, singlet PES.* This two-step oxygen transfer first forms  $\alpha$ -lactone **1** which then fragments to CO + CH<sub>2</sub>O via TS2 (Figure 6). The HF/6-31G\* computed reaction path passes through <sup>1</sup>C<sub>1</sub>, a van der Waals-like complex of <sup>1</sup>:CH<sub>2</sub> + CO<sub>2</sub>, and then over the 9.0 kcal/mol barrier of TS1 to arrive at **1**. At the MP2/6-31G\* level, <sup>1</sup>C<sub>1</sub> and TS1 are no longer stationary points, allowing separate <sup>1</sup>:CH<sub>2</sub> + CO<sub>2</sub> to collapse, without barrier, to  $\alpha$ -lactone **1**. Because of the differences in the results at different levels of theory, we further examined the two structures, <sup>1</sup>C<sub>1</sub> and TS1, using DFT and QCI methods.<sup>26,34</sup> At the B3LYP/6-31G\* level, both structures collapsed to **1**, but

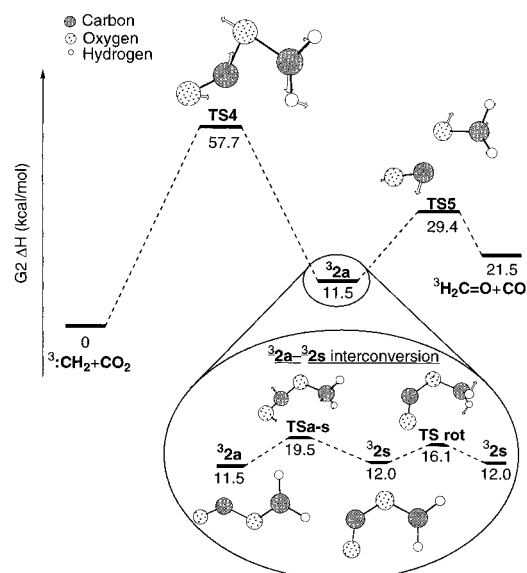


**Figure 5.** Path a on triplet PES. The G2 enthalpies are referenced to <sup>3</sup>:CH<sub>2</sub> + CO<sub>2</sub> as 0 kcal/mol. The geometries of complex <sup>3</sup>2a and the transition states connecting it with starting and ending points of the reactions, TS4 and TS5, respectively, are represented. For TSs, arrows indicate the imaginary vibration which corresponds to the reaction coordinate. The interconversion <sup>3</sup>2a to <sup>3</sup>2s with the corresponding TSa-s and the TSrot for the rotation of <sup>3</sup>2s along the C–O bond is represented separately.

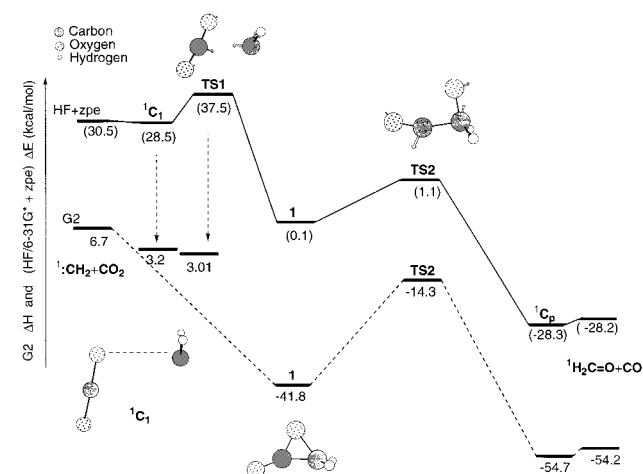


**Figure 6.** Path b on singlet PES. Continuous lines are used for the path calculated at the HF level and dotted lines for G2. The energies are referenced to <sup>3</sup>:CH<sub>2</sub> + CO<sub>2</sub> as 0 kcal/mol. The geometries of  $\alpha$ -lactone **1** and the transition states connecting it with <sup>1</sup>:CH<sub>2</sub> + CO<sub>2</sub>, TS1 and H<sub>2</sub>CO + CO, TS2, respectively, are represented. For TSs, arrows indicate the imaginary vibration which corresponds to the reaction coordinate.

the QCISD/6-31G\* model found <sup>1</sup>C<sub>1</sub> and TS1 respectively to lie 4.3 and 3.0 kcal/mol lower in energy than <sup>1</sup>:CH<sub>2</sub> + CO<sub>2</sub>. G2 single point energies were obtained for the QCISD/6-31G\* geometries of <sup>1</sup>C<sub>1</sub> and TS1, as shown by the dotted arrows in Figure 6.

*path c, triplet PES.* This process forms planar acetoxy diradical <sup>3</sup>3p (Figure 7) when <sup>3</sup>:CH<sub>2</sub> attacks CO<sub>2</sub> at the carbon atom via TS6, after passing through a shallow van der Waals-like complex <sup>3</sup>C<sub>1</sub>. With a G2 calculated barrier of 19.3 kcal/mol, this is the lowest energy triplet reaction path.

Closure of the acetoxy diradical <sup>3</sup>3p to  $\alpha$ -lactone **1** may occur only after ISC to the singlet PES. An optimization of <sup>1</sup>3p, starting at the geometry of <sup>3</sup>3p, directly collapses to  $\alpha$ -lactone **1**.<sup>19</sup>

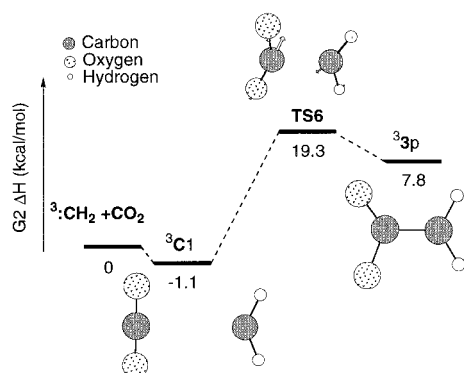


**Figure 7.** Path c on triplet PES. The G2 energies are referenced to  $^3\text{CH}_2 + \text{CO}_2$  as 0 kcal/mol. The geometries of complex  $^3\text{C}_1$  and the transition state connecting it with  $^3\text{CH}_2 + \text{CO}_2$ , **TS6** are represented. For **TS6** arrows indicate the imaginary vibration which corresponds to the reaction coordinate.

Calculations at the HF, MP2, B3LYP, and QCISD/6-31G\* levels yield structures for complex  $^3\text{C}_1$  with C–C distances ranging from 3.5 to 3.2 Å, and energies from 0.6 to 1.1 kcal/mol below  $^3\text{CH}_2 + \text{CO}_2$ . Starting from the MP2 optimized geometry, G2 calculations find an energy only 0.8 kcal/mol lower than the separated species. As with the singlet PES, IRC calculations find  $^3\text{C}_1$  at the dissociation endpoints from both **TS6** and **TS4** (i.e., paths a and c).

**Intermediates.** As noted above, we have examined here  $\alpha$ -lactone **1**, ylide **12**, diradical **32**, and acetoxy diradical **33** (Figure 1). The singlet zwitterionic state of structure **3** was not considered. Although early experimental studies in solution invoked such a dipolar species formed by ring opening of substituted  $\alpha$ -lactones to explain formation of polyester products,<sup>35</sup> calculations by Davidson et al.<sup>19</sup> found the corresponding structure for the parent  $\alpha$ -lactone to be higher in energy than the corresponding diradicals, and to collapse without barrier to **1**.<sup>36</sup>

**Ylide 12 (= TS3).** Despite extensive searching, no conventional  $\text{O}=\text{C}=\text{O}^+ - \text{CH}_2^-$  ylide minimum **12** was located.<sup>4</sup> At all levels of calculation used here, the putative ylide is found to be a TS in **path a**, the one-step oxygen abstraction; it was therefore renamed **TS3**. This result is unsurprising; CO<sub>2</sub> is a weak Lewis base, as evidenced by its low proton and methyl cation affinities, compared to those for CH<sub>2</sub>O (129.2 and 49.4 vs 170.4 and 78.5 kcal/mol, respectively).<sup>37</sup> Its affinity toward singlet methylene would be expected to be substantially lower than the corresponding 46.8 kcal/mol value for formaldehyde.<sup>38</sup>

In our attempt to find a minimum with an ylide-like structure, we ran open shell singlet optimizations, using the UHF/6-31G\* and UMP2/6-31G\* methods, and starting from both the singlet transition state **TS3** and the triplet minimum **32** geometries.<sup>39</sup> Both cases led to structures which are essentially **32**; their geometries match those of **32** and their wave functions yield calculated S<sup>2</sup> values, respectively, of 1.024 and 1.028 which drop to 0.194 and 0.223 after annihilation of the triplet spin contaminant, confirming the essential triplet nature of these structures.

**Diradical 32.** Infrared studies of the reaction of HO• radicals with CO<sub>2</sub><sup>40</sup> indicate the existence of the H–O–CO• species in two conformations, syn and anti. As expected, our calculations find two analogous conformations for the triplet  $\cdot\text{H}_2\text{C}-\text{O}-\text{CO}\cdot$  diradical **32** (Figure 5). The energy differences between syn and anti conformers, **32s** and **32a**, are small at all levels (from 1.8 kcal/mol at the HF/6-31G\* to 0.5 kcal/mol at G2 levels). Barriers of 8.0 and 4.1 kcal/mol (at the G2 level) were found for anti to

**TABLE 4: Estimated Heats of Formation for the Diradical Intermediates**

	$\Delta H_f$ (kcal/mol)	expt <sup>a</sup>	calcd <sup>b</sup>	estimated
	H <sub>3</sub> C–CO–OH	–103.3 ± 0.4	–104.4 <sup>c</sup>	
	H <sub>3</sub> C–CO–O•		–45.0 <sup>c</sup>	
<b>33p</b>	•H <sub>2</sub> C–CO–OH		–56.6 <sup>c</sup>	
	•H <sub>2</sub> C–CO–O•		6.2	2.8 <sup>d</sup>
	H–CO–OCH <sub>3</sub>	–86.6 ± 0.2	–88.3	
	•CO–OCH <sub>3</sub>		–39.8	
<b>32a</b>	H–CO–OCH <sub>2</sub> •		–38.6	
	•CO–OCH <sub>2</sub> •		10.0	13.4 <sup>d</sup>

<sup>a</sup>  $\Delta H_f$  experimental.<sup>37</sup> <sup>b</sup>  $\Delta H_f$  of all species calculated from their heat of atomization using G2 enthalpies and experimental  $\Delta H_f$  of atoms. <sup>c</sup>  $\Delta H_f$  values calculated with our data for the first three species are slightly higher than the G2MP2 values of Rauk et al.<sup>43</sup> <sup>d</sup>  $\Delta H_f$  estimated considering the enthalpies of hydrogen atom loss as additive quantities: for instance, CH<sub>3</sub>–CO–OH → CH<sub>3</sub>–CO–O•,  $\Delta\Delta H_f = +59.4$  kcal/mol (ignoring 1/2H<sub>2</sub> product) and CH<sub>3</sub>–CO–OH → •CH<sub>2</sub>–CO–OH,  $\Delta\Delta H_f = -47.8$  kcal/mol, so  $\Delta H_f$  for **33p** diradical is estimated at 59.4 + 47.8 – 104.4 = 2.8 kcal/mol.

syn conversion (via **TSa**–s) and rotation of the CH<sub>2</sub> moiety (via **TSrot**), respectively.

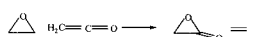
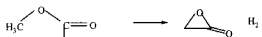

The matrix experiments of Milligan and Jacox located the carbonyl stretches for anti and syn HO–CO• species at 1883 cm<sup>-1</sup> and 1793 cm<sup>-1</sup>, respectively. Our calculations found the corresponding scaled<sup>41,42</sup> vibrations for **32a** at 1811 cm<sup>-1</sup> and for **32s** at 1781 cm<sup>-1</sup> at the MP2/6-31G\* level. These frequencies, substantially lower than those for  $\alpha$ -lactone **1**, reflect the acyclic connectivity in the **32** structures. Similarly, the O–C–O angles of 126.3° and 129.9° for **32a** and **32s** compare well with the corresponding 126.7° and 130.1° values for HOCO• calculated by Rauk et al.<sup>43</sup> As shown in Table 4,  $\Delta H_f$ (**32a**) is calculated to be 10.0 kcal/mol at the G2 level, 3.4 kcal/mol lower than the value obtained by summing the separate enthalpy changes for loss of hydrogen atoms from methyl formate to make a “noninteracting” diradical. This lowering of the energy can be understood as the stabilization due to interaction between the two unpaired electrons in **32a**.

**$\alpha$ -Lactone 1.** The simple product of methylene cycloaddition across a C=O double bond,  $\alpha$ -lactone **1** is characterized here by geometry optimization and vibrational analysis (see Table 2 and Figure 6).<sup>44</sup> The first estimated value available in the literature for the heat of formation of  $\alpha$ -lactone **1**, based on bond additivity, is –31 kcal/mol.<sup>45</sup> Davidson’s ab initio data<sup>19,20</sup> suggest  $\Delta H_f$ (**1**) = –51 kcal/mol. This value was used by Squires to interpret collision-induced dissociation (CID) measurements on chloroacetyl anion.<sup>22</sup> Rodriguez et al. combined QCISD(T) calculations with known heats of formation in two different isodesmic reactions to estimate  $\Delta H_f$ (**1**) = –45.4 ± 2.4 kcal/mol,<sup>23</sup> in good agreement with the improved  $\Delta H_f$ (**1**) = –47.3 ± 4.7 kcal/mol value from Squires et al.<sup>21</sup> Our own estimates,<sup>46</sup> from calculated G2 reaction energies and experimental heats of formation for known species, are shown in Table 5.

The G2 calculated enthalpy of atomization (see Table 5) yields  $\Delta H_f$ (**1**) = –43.3 kcal/mol. However, additional estimates were made via a series of isodesmic reactions, as summarized in Table 5. Taken together, the results suggest that the true  $\Delta H_f$ (**1**) may be slightly higher than the atomization value, but still within the error limits suggested by Rodriguez et al.

Of the three intermediates considered here, **1** is the most stable and is formed through attack of singlet methylene on a C=O  $\pi$  bond of CO<sub>2</sub> in a barrierless process. Ring fragmentation, **1** → CO + H<sub>2</sub>CO, is calculated (G2) to occur via **TS2** with  $\Delta H^\ddagger = 27.5$  kcal/mol and  $\Delta H_{\text{rxn}} = -12.4$  kcal/mol, similar to the 32.2

**TABLE 5: Isodesmic Reactions and Thermodynamic Data for  $\alpha$ -Lactone 1**

$\Delta H_f$ from isodesmic reactions	G2 $\Delta H_{rxn}$	Estimated $\Delta H_f$ (1)
$^1\text{CH}_2 + \text{CO}_2 \rightarrow \text{C}_2\text{H}_2\text{O}_2$	-48.4	-41.1 $\pm$ 0.
$^3\text{CH}_2 + \text{CO}_2 \rightarrow \text{C}_2\text{H}_2\text{O}_2$	-41.8	-43.5 $\pm$ 0.
$\text{CO} + \text{H}_2\text{CO} \rightarrow \text{C}_2\text{H}_2\text{O}_2$	12.4	-41.7 $\pm$ 0.
$\text{CO} + ^3\text{H}_2\text{CO} \rightarrow \text{C}_2\text{H}_2\text{O}_2$	-63.2	-43.4 $\pm$ 0.04
	-4.96	-41.5 $\pm$ 0.75
	42.51	-43.2 $\pm$ 0.20
	58.60	-41.1 $\pm$ 0.10
$\Delta H_f$ from $\Delta H_{atomization}^b$	G2 $\Delta H_f$	Experimental $\Delta H_f^c$
$2\text{C} + 2\text{H} + 2\text{O} \rightarrow \text{C}_2\text{H}_2\text{O}_2$ ( $\alpha$ -lactone)	-43.3	
$2\text{H} \rightarrow \text{H}_2$	-1.1	0.0
$\text{C} + 2\text{H} \rightarrow ^1\text{CH}_2$	101.4	101.35
$\text{C} + 2\text{H} \rightarrow ^3\text{CH}_2$	94.8	92.35
$\text{C} + \text{O} \rightarrow \text{CO}$	-28.0	-26.42 $\pm$ 0.04
$\text{C} + 2\text{O} \rightarrow \text{CO}_2$	-96.3	-94.05 $\pm$ 0.03
$\text{C} + 2\text{H} + \text{O} \rightarrow \text{H}_2\text{CO}$	-27.7	-27.70
$\text{C} + 2\text{H} + \text{O} \rightarrow ^3\text{H}_2\text{CO}$	47.9	46.2
$2\text{C} + 4\text{H} \rightarrow \text{C}_2\text{H}_4$ (ethylene)	12.9	12.54
$2\text{C} + 4\text{H} + \text{O} \rightarrow \text{C}_2\text{H}_4\text{O}$ (oxirane)	-13.8	-12.58 $\pm$ 0.15
$2\text{C} + 2\text{H} + \text{O} \rightarrow \text{CH}_2\text{CO}$	-11.8	-11.40 $\pm$ 0.40 <sup>c</sup>
$2\text{C} + 2\text{H} + \text{O} \rightarrow \text{HCOOCH}_3$	-88.3	-86.60 $\pm$ 0.20
$2\text{C} + 2\text{H} + \text{O} \rightarrow \text{CH}_3\text{COOH}$	-104.4	-103.30 $\pm$ 0.40

<sup>a</sup> Experimental  $\Delta H_f$ .<sup>31,37</sup> <sup>b</sup>  $\Delta H_f$  calculated from the corresponding heats of atomization with G2 enthalpy<sup>29</sup> and experimental  $\Delta H_{f,atom}$  values for the elements as follows: G2 enthalpy (in Hartrees), H = 627.5 kcal/mol, experimental  $\Delta H_f$  (kcal/mol), H: -0.58067, 52.1; O: -75.07445, 59.6; C<sub>gas</sub>: -38.05482, 171.3. <sup>c</sup> Of the three values listed in the NIST database for ketene's heat of formation, we selected the one closest to our calculated value. The experimental  $\Delta H_f$  values compare well with the calculated ones at G2, with an average difference of  $\pm 1.03$  kcal/mol.

and -12.2 kcal/mol MP2/6-31G\*\* values obtained by Domingo et al.<sup>24</sup> in their theoretical study of gas-phase  $\alpha$ -hydroxyacid decarboxylation. These  $\Delta H_{rxn}$  values differ from Liebman's -23.4 kcal/mol estimated exothermicity<sup>45</sup> as expected, given the above adjustments in the estimated  $\Delta H_f$  of  $\alpha$ -lactone. Ring-opening (**path b**) to zwitterionic intermediates has been proposed to explain polyester products in solution studies of  $\alpha$ -lactone-forming reactions.<sup>35</sup> However, as noted below, all singlet biradical structures we examined fragmented or collapsed to **1** upon optimization. Thus, **1** represents a fairly deep potential energy well, and should be easily observed at sufficiently low temperatures.

The IR data attributed by Milligan and Jacox to **1**, matrix isolated in Ar, show  $^{12}\text{C}=\text{O}$  and  $^{13}\text{C}=\text{O}$  carbonyl stretches at 1967 and 1933  $\text{cm}^{-1}$ , respectively, with the abnormally high frequency attributed to the strain in the  $\alpha$ -lactone ring. Our scaled values for **1** (1974 and 1919  $\text{cm}^{-1}$  at HF/6-31G\*; 1927 and 1873  $\text{cm}^{-1}$  at MP2/6-31G\* levels,<sup>41,42</sup> respectively) match these experimental results rather well, deviating less than they do for formaldehyde.<sup>47</sup> Of the possible intermediates considered here, only **1** has a strong vibration located near the experimental value. The other candidates, **32** and **33**, also have C=O stretch vibrations, but at lower frequencies (1879 and 1667  $\text{cm}^{-1}$ , respectively, at the HF/6-31G\* level).

The triplet  $\alpha$ -lactone excited state, **31**, was examined as part of our exploration of the triplet PES and ISC possibilities. The HF/6-31G\* structure lies 60.3 kcal/mol higher in energy than the corresponding singlet and shows substantial pyramidalization at the carbonyl carbon; the MP4/6-31G\*\*/HF/6-31G\* energy difference is even larger (90 kcal/mol). Upon reoptimization at the MP2/6-31G\* level, the ring opens via C-C cleavage to form

the diradical **32a**, 53.3 kcal/mol higher in energy than **1** at the G2 level. These results indicate that **31** is energetically out of reach and therefore unlikely to play any role in the title reaction.

**Acetoxy Diradical 33.** Addition of  $^3\text{CH}_2$  to the carbon of  $\text{CO}_2$  leads to **33**, the acetoxy diradical, which has been computationally analyzed in the literature,<sup>19</sup> in a somewhat different context. Using the 6-31G\* basis set (compared with 3-21G+d+sp from ref 19), we found the two reported structures, planar **33p** and staggered **33s**. At the MP2 and HF levels, only the planar diradical is a minimum. The planar and staggered structures **33** are higher in energy than  $^3\text{CH}_2 + \text{CO}_2$  by 7.8 and 16.3 kcal/mol (G2), respectively. Geometrical data compare well with reported MP2/6-31G\* structures<sup>41</sup> of monoradicals  $\text{CH}_3-\text{CO}-\text{O}\cdot$  and  $\cdot\text{CH}_2-\text{COOH}$ .  $\Delta H_f$  data from the same source were used (Table 4) to calculate  $\Delta H_f$  of diradicals **33**. Unlike for the case of **32a**, the value predicted using additivity, 2.8 kcal/mol, is lower than the 6.2 kcal/mol calculated from G2 heats of atomization, suggesting that in this case, the two unpaired electrons interact to raise the energy of the entire entity.

The acetoxy diradical was recently studied<sup>22</sup> by tandem mass spectrometry and by energy resolved collisional induced dissociation. From the appearance energy measurements, a gap of 2 kcal/mol was estimated between the triplet and its lowest singlet state. The triplet lowest energy path is decomposition to  $^3\text{CH}_2 + \text{CO}_2$  while the open shell singlet is thought to easily evolve to "hot"  $\alpha$ -lactone which, in turn, decomposes to form the observed  $\text{CO} + \text{H}_2\text{CO}$  products.

Of the two possible  $^3\text{CH}_2 + \text{CO}_2$  adducts, **33p** and **32a**, the former is both lower in energy (by 3.7 kcal/mol) and accessible via a lower barrier (19.3 vs 57.7 kcal/mol via **TS6** vs **TS4**, respectively, Figure 3). But unless it isomerizes to **32** or closes to  $\alpha$ -lactone **1**, **33p** cannot complete the oxygen transfer of interest here. Formation of  $^3\text{CH}_2\text{O}$  and  $\text{CO}$  would require isomerization over a high barrier (84.9 kcal/mol via **TS7**, found only at the HF/6-31G\* level<sup>48</sup>) to **32a**, before cleavage to  $^3\text{CH}_2\text{O} + \text{CO}$  via **TS5**, which itself has a barrier of 17.9 kcal/mol (G2). Thus  $^3\text{CH}_2 + \text{CO}_2$  might react at thermal energies to form acetoxy diradical **33**, but this intermediate's principle choice would be to redissociate to  $^3\text{CH}_2 + \text{CO}_2$  or undergo ISC to the singlet surface, followed by barrierless closure to **1**.

Comparing the available singlet and triplet data, the region of the PES surrounding species **3** appears well suited for intersystem crossing (ISC). Single-point singlet state energy calculations for the **3p** and **3s** structures find **13s** to be much lower in energy than the corresponding triplet and even lower than the energy of starting  $^1\text{CH}_2 + \text{CO}_2$  (Figure 8). As expected, optimization on the singlet surface starting from the geometry of **33s** ( $C_s$  symmetry) led directly to  $\alpha$ -lactone **1**, as found by Davidson.<sup>19</sup> Singlet optimization ( $C_s$  symmetry) from the analogous planar geometry **33p** leads to a transition structure for  $\cdot\text{H}_2\text{C}-\text{CO}_2\cdot$  bond rotation. Rotation from planar acetoxy diradical **33p** to staggered **33s**, a TS, offers a possible channel for ISC from the triplet **33p** to the singlet **13s** which would then collapse to  $\alpha$ -lactone.

**Intersystem Crossing.** Our calculations agree well with the literature's structural and spectroscopic results. But the correspondence between experiment and theory is less satisfactory for the available kinetic data.<sup>7,8,11,12</sup> Singlet methylene is the primary photolysis product from all the precursors studied to date, but with  $\text{CO}_2$ , it is collisionally deactivated to the triplet state twice as fast as it reacts.<sup>11,12</sup> The reaction of triplet methylene with  $\text{CO}_2$  is slower than the singlet methylene reaction, in qualitative agreement with our results. However, the rate difference is only a factor of ca. 1000. Assuming even

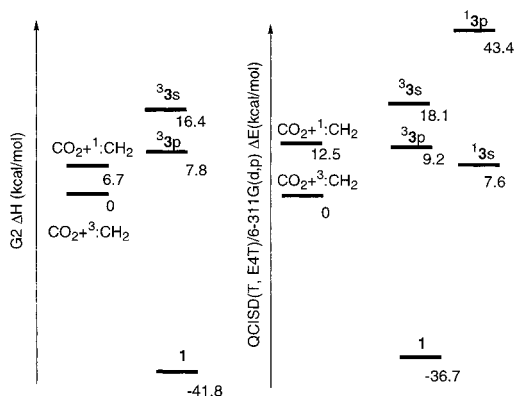


**Figure 8.** The energy levels of  $^3\text{p}$ ,  $^3\text{s}$ , and  $^1$  species, referenced to  $^3\text{:CH}_2 + \text{CO}_2$  considered as 0 kcal/mol, at G2 and QCISD/6-31G\*//QCISD/6-31G\* levels. At the QCISD level the singlet spin calculations indicate  $^1\text{s}$  lower in energy than both  $^3\text{p}$  and  $^3\text{s}$  and even lower than  $\text{CO}_2 + ^1\text{:CH}_2$ , on the singlet PES.

vaguely similar Arrhenius preexponential factors (within a factor of  $\pm 100$ ) for the singlet and triplet reactions, the activation energy difference at ambient temperature would only be in the 3–6 kcal/mol range, substantially below the 9 kcal/mol singlet–triplet gap in methylene. Since all attack paths on the triplet PES are endothermic, the apparently excessive rate constant for the reaction of  $^3\text{:CH}_2$  with  $\text{CO}_2$  suggests that in the collision complex, the singlet PES must begin to fall as the triplet PES begins rising, allowing intersystem crossing up to the singlet surface at energies lower than separated  $^1\text{:CH}_2 + \text{CO}_2$ . Such nonequilibrium intersystem crossings have been extensively discussed for the condensed phase reaction of diphenylmethane with methanol.<sup>49</sup> The crossing of interest in the present system would represent the intersection of **path c** (triplet) with **path b** (singlet) before **TS6** is reached.

Without reasonably well balanced descriptions of the singlet and triplet electronic states, it is problematic to directly search for surface crossings, especially in a polyatomic system. We therefore resorted first to simple QCISD/6-31G\* vertical excitation calculations, in which geometries calculated from one spin state's PES were used to compute the other spin state's energy without further optimization. The corresponding vertical excitation energies for the separated  $\text{:CH}_2$  (+ ground-state  $\text{CO}_2$ ) systems were used as reference points. We examined complexes  $^3\text{C}_1$  and  $^1\text{C}_1$ , the two points earliest in the  $\text{CH}_2\text{--CO}_2$  approach paths. For the  $^3\text{C}_1$  geometry<sup>26</sup> the QCISD/6-31G\* S–T gap is 1.6 kcal/mol smaller than that found for the geometry of  $^3\text{:CH}_2$ , suggesting that the surfaces are approaching each other. Consistent with this notion is the finding that for the  $^1\text{C}_1$  geometry, the triplet QCISD/6-31G\* energy is 7.6 kcal/mol above that of  $^1\text{C}_1$ . The calculated S–T gap for methylene ( $^1\text{:CH}_2$  geometry) places  $^3\text{:CH}_2$  5.0 kcal/mol below  $^1\text{:CH}_2$ . The implication is that at some intermediate geometry en route to  $^1\text{C}_1$ , the singlet and triplet surfaces must have crossed, albeit at an energy higher than separated triplet reactants.

A direct search for crossings between the singlet and triplet PESs was carried out using the conical intersection searching routine in Gaussian 98.<sup>50</sup> This calculation used a CASSCF(6,6)/6-311+G(3df,2p) wave function, which correlated the two nonbonding orbitals ( $\text{sp}^2$  and  $\text{p}$ ) on  $\text{CH}_2$ , and the two sets of degenerate  $\pi$  and  $\pi^*$  orbitals ( $\pi_x$  and  $\pi_y$ ) on  $\text{CO}_2$ . Unfortunately, energy gaps obtained for the resulting structure at the G2 and explicit QCISD(T)/6-311+G(3df,2p) levels remained significant, with the singlet energies 6.6 and 4.1 kcal/mol below the triplet, respectively. For reference, methylene's S–T gap at the QCISD(T)/6-311+G(3df,2p)/MP2/6-31G\* level (with thermal correc-

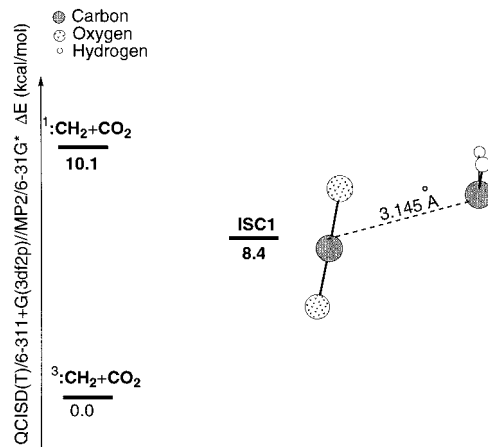


**Figure 9.** Surface crossing region. The energies are referenced to  $^3\text{:CH}_2 + \text{CO}_2$  as 0 kcal/mol. The geometry of surface crossing structure, **ISC1** resembles  $^1\text{C}_1$  with a C–C distance 1.345 Å and a HCH methylene angle of  $109.6^\circ$ .

tions taken from the G2 calculation) is 10.1 kcal/mol. The above discrepancy may be attributed to the fact that the conical intersection procedure calculates a mixed state with a wave function different from either of the pure singlet or triplet states.

Unsatisfied by our attempts at direct optimization, we elected to search by hand for the minimum energy crossing point of the singlet and triplet reaction surfaces using explicit QCISD(T)/6-311+G(3df,2p) energies. It is this level of theory that the G2 method is designed to approximate. For the relatively small  $\text{CH}_2 + \text{CO}_2$  system, the explicit calculation is accessible, and its calculated S–T gap for  $\text{CH}_2$  is substantially closer than G2's to the experimental value (10.1 kcal/mol vs G2's 6.7; expt. = 9.0 kcal/mol). As a starting point, we obtained the lowest surface crossing geometry for isolated  $\text{CH}_2$  by searching the two-dimensional grid of C–H bond length and HCH angle. This  $\text{CH}_2$  geometry, which is very close to the singlet minimum, was held fixed and allowed to interact in the triplet state with a  $\text{CO}_2$  molecule. The resulting structure, which was similar to  $^1\text{C}_1$ , was used as a starting point for further hand optimizations.

Analytically calculated singlet and triplet MP2/6-31G\* optimization step displacements were scaled by their projected energy lowerings, summed, scaled typically by a factor of 0.25, and used to generate new geometries for which the expected singlet and triplet QCISD(T)/6-311+G(3df,2p) energies would be equal. Since  $^1\text{:CH}_2$  falls monotonically to the  $\alpha$ -lactone minimum at the MP2/6-31G\* level, and the widening of the HCH angle relaxes  $^3\text{:CH}_2$ , energy-lowering distortions were available for each of the two states. Although the procedure for achieving compromise required some experimentation, we succeeded in lowering the overall energy, while keeping the S–T gap close, by balancing these structural driving forces for the two systems. After thermal corrections, the resulting structure **ISC1** lay 1.7 kcal/mol lower in energy than the separated  $^1\text{:CH}_2 + \text{CO}_2$ , indicating that a lowering of the effective  $^3\text{:CH}_2 + \text{CO}_2$  reaction barrier by at least this amount is possible. Its geometry is similar to that of  $^1\text{C}_1$  with the two carbon atoms at a distance of 1.345 Å and an HCH angle of  $109.6^\circ$  (see Figure 9). Evaluation of spin–orbit coupling (CASSCF(6,6)/6-311+G(3df,2p) wave functions) at the crossing point geometries, found with both conical intersection and hand searches, yielded essentially identical values of 13.6 and 13.4  $\text{cm}^{-1}$ , respectively. An analogous search for a crossing region in the transverse or higher symmetry approaches to  $\text{CO}_2$  yielded nothing of interest; no monotonically exothermic cycloaddition by  $^1\text{C}_1$  is available

in these approach arrangements. Thus, all the above efforts confirm that as  $\text{:CH}_2$  approaches  $\text{CO}_2$ , the singlet PES descends to meet the rising triplet PES, allowing the crossing from the triplet to the singlet surface and the resulting formation of  $\alpha$ -lactone.

## Conclusions

Abstraction of oxygen by  $\text{:CH}_2$  from  $\text{CO}_2$  appears to occur via stepwise processes, despite the 61 kcal/mol overall exothermicity of this reaction. Singlet methylene attack on the  $\pi$  bond of  $\text{CO}_2$  to form  $\alpha$ -lactone was found to be the most favorable process on the singlet potential energy surface, much like the familiar barrierless concerted cycloaddition of methylene to alkenes. Under low-pressure conditions, this reaction's 47.5 kcal/mol exothermicity is more than enough to complete the net O-transfer via fragmentation of the vibrationally hot lactone into CO and  $\text{CH}_2\text{O}$ . With its high frequency ( $\sim 1900\text{ cm}^{-1}$ ) carbonyl stretch, the  $\alpha$ -lactone intermediate has also been experimentally observed in matrix isolation experiments, as have several substituted analogues. Our calculations assign it a heat of formation of  $-43.3 \pm 2$  kcal/mol and find a barrier of 27.5 kcal/mol for its thermal cleavage to  $\text{CH}_2\text{O}$  and CO.

The initially sought one-step oxygen atom abstraction path was also found but with its 23.2 kcal/mol G2 activation barrier, this process is unlikely to play a significant role at common reaction temperatures. Importantly, no minimum was found for a carbonyl ylide-like adduct of  $\text{:CH}_2$  and  $\text{CO}_2$ . This finding appears at odds with a previous report from a matrix isolation study of 4-biphenylchlorocarbene +  $\text{CO}_2$ ,<sup>4</sup> but perhaps ylide formation is favored by the different carbene substituents and the condensed phase environment of the experiment.

On the triplet PES, the lowest energy attack occurs at the  $\text{CO}_2$  carbon (**path c**) over a 19.3 kcal/mol barrier to form acetoxyl diradical **33**; attack at oxygen (**path a**) to form **32** has an even higher barrier, 57.7 kcal/mol. The lowest energy path available to **33** is to fragment back to  $\text{CO}_2$  and  $\text{:CH}_2$ , but this species could function as a possible intermediate in the net oxygen transfer via ISC (to **path b**), collapse to  $\alpha$ -lactone **1**, and subsequent fragmentation on the singlet PES. However, both of these triplet attack barriers substantially exceed the 9 kcal/mol S–T gap in methylene, so the most thermochemically accessible path for the  $\text{:CH}_2 + \text{CO}_2$  reaction (disregarding surface crossings; vide infra) would be via reequilibration to the singlet state, either alone or assisted by collision with  $\text{CO}_2$ . Thus, the net oxygen transfer is unlikely to involve contributions from any reaction steps on the pure triplet PES.

According to our calculations, the nature of the attack depends on the electronic state of the carbene, as expected from the findings of Wagner et al.<sup>11</sup> and seemingly at odds with the philicity-dominated suggestion of Sander et al.<sup>14,15</sup> However, since philicity is defined in terms of a carbene's substrate selectivities, rather than the absolute reactivity (i.e., rate constants) of the carbene's more reactive singlet state, this may be a less significant discrepancy than it appears at first, and one that is resolved by the notion of nonequilibrium surface crossing. The singlet prefers attack on the  $\pi$  system of  $\text{CO}_2$  with the formation of  $\alpha$ -lactone **1** in a barrierless process (**path b**), whereas the triplet likely begins to attack at the carbon atom as a radical (**path c**) but ultimately crosses over to the singlet PES (**path b**) again leading to lactone formation with a lower barrier/faster rate than expected from the simple methylene S–T gap. Since the singlet reaction path of the carbene is accessed even from the triplet PES, it is this philicity-defining state that also determines the relative reactivities with the  $\text{CO}_2$ .

**Acknowledgment.** The authors gratefully acknowledge both specific helpful comments on this work and the overall encouragement offered by Bob Squires before his untimely death. His science and life continue to provide inspiration to organic and mechanistic chemists, and we sorely miss him. We also gratefully acknowledge the National Science Foundation for funds (CHE-9974834) to purchase a new departmental supercomputer system.

**Supporting Information Available:** A complete summary with Cartesian coordinates and calculated enthalpies for all the species discussed is available as supporting material. This material is available free of charge via the Internet at <http://pubs.acs.org>.

## References and Notes

- (1) Kistiakowsky, G. B.; Sauer, K. *J. Am. Chem. Soc.* **1958**, *86*, 1066.
- (2) Kovacs, D.; Lee, M.-S.; Olson, D.; Jackson, J. E. *J. Am. Chem. Soc.* **1996**, *118*, 1844.
- (3) (a) Jackson, J. E.; Mock, G. B.; Tetef, M. L.; Zheng, G.-X.; Jones, M., Jr. *Tetrahedron* **1985**, *41*, 1453; (b) Jackson, J. E.; Misslitz, U.; Jones, M., Jr.; De Meijere, A. *Tetrahedron* **1987**, *43*, 653.
- (4) Personal communication: Naito, I.; Mizo, T.; Kobayashi, S.; Matsumoto, T.; Oku, A. Reported laser flash photolysis of (biphenyl-4-yl)chlorodiazirine in  $\text{CO}_2$ -saturated acetonitrile, a short-lived species, with UV absorption at ca. 510 nm, is suggested to be the ylide formed by the attack of carbene on one of the oxygen atoms of  $\text{CO}_2$ .
- (5) Milligan, D. E.; Jacox, M. E. *J. Chem. Phys.* **1962**, *36*, 2911.
- (6) For  $\text{CH}_2\text{N}_2 + \text{CO}_2$  1967  $\text{cm}^{-1}$ ;  $\text{CD}_2\text{N}_2 + \text{CO}_2$  1961  $\text{cm}^{-1}$ ;  $\text{CH}_2\text{N}_2 + {}^{13}\text{CO}_2$  1933  $\text{cm}^{-1}$ .
- (7) Laufer, A. H.; Bass, A. M. *Chem. Phys. Lett.* **1977**, *46*, 151.
- (8) According to recent measurements, this reaction has an upper limit of  $k = 10^{-14}\text{ cm}^3\text{ molecule}^{-1}\text{ s}^{-1}$ ; see Darwin, D. C.; Moore, C. B. *J. Phys. Chem.* **1995**, *99*, 13467.
- (9) Hsu, D. S.; Lin, M. C. *Int. J. Chem. Kinet.* **1977**, *IX*, 507.
- (10) Shortridge, R. G.; Liu, M. T. *J. Chem. Phys.* **1976**, *64*, 4076.
- (11) Koch, M.; Temps, F.; Wagener, R.; Wagner, H. Gg. *Ber. Bunsen-Ges. Phys. Chem.* **1990**, *94*, 645.
- (12) Böhlend, T. Unpublished results, cited in ref 11.
- (13) DeMore, W. B.; Pritchard, H. O.; Davidson, N. *J. Am. Chem. Soc.* **1959**, *81*, 15874.
- (14) Sander, W. W. *J. Org. Chem.* **1989**, *54*, 4265.
- (15) Sander, W. W.; Patyk, A.; Bucher, G. *J. Mol. Struct.* **1990**, *222*, 21.
- (16) Wierlacher, S.; Sander, W.; Liu, M. T. H. *J. Org. Chem.* **1992**, *57*, 1051.
- (17) Triplet carbenes: diphenylcarbene and cyclohexadienylidene; Singlet carbenes: phenyl chlorocarbene and *p*-nitrophenyl chlorocarbene.
- (18) Chateaufneuf, J. E. *Res. Chem. Intermed.* **1994**, *20*, 159.
- (19) Antolovic, D.; Shiner, V. J.; Davidson, E. R. *J. Am. Chem. Soc.* **1988**, *110*, 1375.
- (20) The calculations reported in ref 19 were performed using HF and CISD 3-21G+d+sp and D95+d+sp wave functions.
- (21) Graul, S. T.; Squires, R. R. *Int. J. Mass Spectrom. Ion Processes* **1990**, *100*, 785.
- (22) Schroder, D.; Goldberg, N.; Zummack, W.; Schwarz, H.; Poutsma, J. C.; Squires, R. R. *Int. J. Mass Spectrom. Ion Processes* **1997**, *165*, 71.
- (23) Rodriguez, C. F.; Williams, I. H. *J. Chem. Soc., Perkin Trans. 2* **1997**, 953.
- (24) Domingo, R. L.; Andres, J.; Moliner, V.; Safont, V. S. *J. Am. Chem. Soc.* **1997**, *119*, 6415.
- (25) Frisch, M. J.; Trucks, G. W.; Schlegel, H. B.; Gill, P. M. W.; Johnson, B. G.; Robb, M. A.; Cheeseman, J. R.; Keith, T. A.; Peterson, G. A.; Montgomery, J. A.; Raghavachari, K.; Al-Laham, M. A.; Zakrzewski, V. G.; Ortiz, J. V.; Foresman, J. B.; Cioslowski, J.; Stefanov, B. B.; Nanayakkara, A.; Challacombe, M.; Peng, C. Y.; Ayala, P. Y.; Chen, W.; Wong, M. W.; Andres, J. L.; Replogle, E. S.; Gomperts, R.; Martin, R. L.; Fox, D. J.; Binkley, J. S.; Defrees, D. J.; Baker, J.; Steward, J. P.; Head-Gordon, M.; Gonzales, C.; Pople, J. A. *Gaussian 94* (Revision D.3); Gaussian, Inc.: Pittsburgh, PA, 1995.
- (26) Detailed geometry and energy data for the species considered are available as supporting material.
- (27) Foresman, J. B.; Frisch, A. *Exploring Chemistry with Electronic Structure Methods: A Guide to Using Gaussian*; Gaussian, Inc.: Pittsburgh, PA, 1993.
- (28) Experimental methylene S–T gap is 9 kcal/mol; see Leopold, D. G.; Murray, K. K.; Miller, A. E. S.; Lineberger, W. C. *J. Chem. Phys.* **1985**, *83*, 4849, or Bunker, P. R.; Jensen, P.; Kraemer, W. P.; Beardsworth,



R. *J. Chem. Phys.* **1986**, *85*, 3724 and references therein. The calculated values at the HF/6-31G\* and MP2/6-31G\* levels are 30 and 21 kcal/mol, respectively.

(29) Curtis, L. A.; Raghavachari, K.; Trucks, G. W.; Pople, J. A. *J. Chem. Phys.* **1991**, *94*, 7221.

(30) Although well-defined economical methods are available for accurate calculations of carbene S–T gaps, their general extrapolation to reaction potential energy surfaces is nontrivial; see Carter, E. A.; Goddard, W. A. *J. Phys. Chem.* **1988**, *88*, 1752.

(31) Lias, S. G.; Bartmess, J. E.; Liebman, J. F.; Holmes, J. L.; Levin, R. D.; Mallard, W. G. Gas-Phase Ion and Neutral Thermochemistry. *J. Phys. Chem. Ref. Data* **1988**, *17*, Suppl. 1.

(32) Yamamoto, N.; Bernardi, F.; Bottoni, A.; Olivucci, M.; Robb, M. A.; Wilsey, S. *J. Am. Chem. Soc.* **1994**, *116*, 2064 and references therein.

(33) The active vibration, corresponding to the reaction coordinate, is indicated by the arrows. This motion leads from the TS toward the reactants or products with which it is connected on PES (see the energy profiles).

(34) We used here the hybrid B3LYP functional (see Becke, A. D. *J. Chem. Phys.* **1993**, *98*, 5648). For the QCISD method, see Pople, J. A.; Head-Gordon, M.; Raghavachari, K.; Trucks, G. W. *Chem. Phys. Lett.* **1989**, *164*, 185.

(35) (a) Wheland, R.; Bartlett, P. D. *J. Am. Chem. Soc.* **1970**, *92*, 6057; (b) Adam, W.; Rucktaschel, R. *J. Am. Chem. Soc.* **1971**, *93*, 557; (c) Chapman, O. L.; Wojtkowski, P. W.; Adam, W.; Rodriguez, R.; Rucktaschel, R. *J. Am. Chem. Soc.* **1972**, *94*, 1365.

(36) Experimental data on solution chemistry of substituted  $\alpha$ -lactone are cited as *Doctoral Dissertation*, McMullen D. F., Indiana University, 1982 in ref 19; the use of water and ethanol/water as solvents allowed isotope effect measurements in the 3-methyl- $\alpha$ -lactone ring opening and suggested a zwitterionic intermediate which easily decomposed into ethylene and CO<sub>2</sub>.

(37) (a) Hunter, E. P.; Lias, S. G. Proton Affinity Evaluation. In *NIST Chemistry Webbook, NIST Standard Reference Database Number 69*; Mallard, W. G., Lindstrom, P. J., Eds.; March 1998, National Institute of Standards and Technology, Gaithersburg, MD, 20899 (<http://webbook.nist.gov>). (b) McMahan, T. B.; Heinis, T.; Nicol, J. K.; Hovey, P.; Kebarle, P. *J. Am. Chem. Soc.* **1988**, *110*, 7591.

(38) Yamaguchi, Y.; Schaefer, H. L., III; Alberts, I. L. *J. Am. Chem. Soc.* **1993**, *115*, 5790.

(39) Considering the limitations of UMP2 method usage, strict interpretation of these results may be misleading. For a discussion of the use of

UMP methods on diradicals see also Jarzecki, A. A.; Davidson, E. R. *J. Phys. Chem. A* **1998**, *102*, 4742.

(40) Milligan, D. E.; Jacox, M. E. *J. Chem. Phys.* **1971**, *54*, 927.

(41) Pople, J. A.; Krishnan, R.; Schlegel, H. B.; DeFrees, D.; Brinkley, J. S.; Frisch, M. J.; Whiteside, R. F.; Hout, R. F.; Hehre, W. J. *Int. J. Quantum Chem. Symp.* **1981**, *15*, 269.

(42) Hehre, W.; Radom, L.; Schleyer, P. R. v; Pople, J. A. *Ab initio molecular orbital theory*; John Wiley and Son: New York, 1986; p 233.

(43) Yu, D.; Rauk, A.; Armstrong, D. A. *J. Chem. Soc., Perkin Trans. 2* **1994**, 2207.

(44) For a review about stable  $\alpha$ -lactones see L'abee G. *Angew. Chem., Int. Ed. Engl.* **1980**, *19*, 276 and references therein.

(45) Liebman, J. F.; Greenberg, A. *J. Org. Chem.* **1974**, *39*, 123.

(46) For a  $\alpha$ -lactone ring opening similar to **TS2** see ref 24, Table 6, p 6420. The cited C–C distance is 1.506 Å vs 1.500 Å in the structure optimized here, at the MP2/6-31G\* level.

(47) For comparison we used the formaldehyde carbonyl stretch. It is 1804 or 1715 cm<sup>-1</sup> computed and scaled at the HF/6-31G\* or MP2/6-31G\* levels, respectively, with a deviation of  $\Delta\nu = +58$  or  $-31$  cm<sup>-1</sup> from the 1746 cm<sup>-1</sup> experimental value.<sup>14</sup>

(48) Despite much effort, no **TS7**-like structure was found at higher levels, suggesting that **TS7** may be an artifact due to the limitations of the HF theory used.

(49) Platz, M. S. *Kinetics and Spectroscopy of Carbenes and Biradicals*; Plenum Press: New York, 1990; p 320.

(50) Frisch, M. J.; Trucks, G. W.; Schlegel, H. B.; Scuseria, G. E.; Robb, M. A.; Cheeseman, J. R.; Zakrzewski, V. G.; Montgomery, J. A.; Stratmann, R. E.; Burant, J. C.; Dapprich, S.; Millam, J. M.; Daniels, A. D.; Kudin, K. N.; Strain, M. C.; Farkas, O.; Tomasi, J.; Barone, V.; Cossi, M.; Cammi, R.; Mennucci, B.; Pomelli, C.; Adamo, C.; Clifford, S.; Ochterski, J.; Petersson, G. A.; Ayala, P. Y.; Cui, Q.; Morokuma, K.; Malick, D. K.; Rabuck, A. D.; Raghavachari, K.; Foresman, J. B.; Cioslowski, J.; Ortiz, J. V.; Stefanov, B. B.; Liu, G.; Liashenko, A.; Piskorz, P.; Komaromi, I.; Gomperts, R.; Martin, R. L.; Fox, D. J.; Keith, T.; Al-Laham, M. A.; Peng, C. Y.; Nanayakkara, A.; Gonzalez, C.; Challacombe, M.; Gill, P. M. W.; Johnson, B. G.; Chen, W.; Wong, M. W.; Andres, J. L.; Head-Gordon, M.; Replogle, E. S.; Pople, J. A. *Gaussian 98 (Revision A.7)*; Gaussian, Inc.: Pittsburgh, PA, 1998.